ORIGINAL ARTICLE

Study on pyrolysis characteristics and kinetics of mixed plastic waste

Fengfu Yin[1] · Qianxiao Zhuang[1] · Tianhao Chang[1] · Chao Zhang[1] · Huadong Sun[1] · Qikun Sun[1] · Chuansheng Wang[1] ·
Lin Li[1]

Abstract

Different types of plastic wastes have caused serious environmental problems. Co-pyrolysis and separation techniques are being widely used because of the complex components of plastic wastes. In this study, Thermogravimetric Analysis for mixed plastics with different compositions (Polypropylene/Polyvinyl chloride and Polypropylene/Polyvinyl chloride/Polystyrene mixtures) was carried out under three heating rates. Aiming at the complex pyrolysis reaction process of mixed plastics, a model-free method and a model-fitting method were combined to obtain the complete kinetics, which makes the results more reliable. The activation energy of the mixture pyrolysis process was carried out by the model-free method, and two stages of pyrolysis mechanism functions were summarized in the model-fitting method. Verification test proves that the mechanism function of this research can be reliable to express the pyrolysis reaction process. This research can provide support for the optimization of pyrolysis process parameters and the design of pyrolysis reactors for chlorine-containing mixed plastics.

Keywords Plastic wastes · Co-pyrolysis · Pyrolysis kinetics · Activation energy

Introduction

In 2018, the global output of plastic reached nearly 360 million tons [1]. The wide use of plastic products provides conveniences for everyday life and industrial production [2, 3]. However, some single-use plastic products, especially those used in the delivery and e-commerce industries, degrade very poorly when they become scrap, posing a huge potential threat to the survival of marine organisms and human health unless some method can be found for processing them [4–7]. As a major producer, consumer and recycler of plastic, China's annual consumption ranks first in the world. Although China's output of plastic products slowed to 60.42 million tons in 2018 due to the impact of the ban on trash import, the recycling rate of plastic is still only 30%, according to the National Bureau of Statistics [8].

Plastics are made primarily from petroleum, a non-renewable resource. In the long run, the recycling of waste plastic has great potential for countries poor in oil resources [9,

10]. Traditional methods of disposal of plastic waste, such as incineration and landfilling, have been banned because of their low recycling efficiency and their tendency to cause secondary pollution [11, 12]. Mechanical recycling is a treatment where waste plastics are extruded and blended with virgin polymers, but the quality of the reprocessed product is very sensitive to the type of virgin polymers. Chemical treatment methods involve chemical and thermal agents to alter the polymeric structure of the finished product [2]. Pyrolysis as a more environmentally friendly and efficient recycling technology decomposes plastic into three valuable fractions: gas, crude oil, and solid residue at relatively moderate temperatures ranging between 770 and 920 K, with tars yields ranging between 75 and 80wt% [13, 14]. These valuable fractions can be obtained in different proportions by the appropriate choice of thermal treatment, degradation temperature, type of plastics, degradation time, and catalyst type, which has become the research direction of plastic waste treatment [15–17].

During the pyrolysis process of PVC and chlorine-containing mixed plastic, the release of PVC has a toxic HCL to corrode the instrument. The chlorine element stays for a long time in the high-temperature environment of pyrolysis, which can result in the formation of unwanted chlorine organic compounds [18]. It largely restricts the application

✉ Lin Li
ll@qust.edu.cn

1 College of Electromechanical Engineering, Qingdao University of Science and Technology, Qingdao 266061, China

of pyrolysis technology in the treatment of chlorine plastic. Therefore, in the pyrolysis process, a special dechlorination process is inquired, so that the chlorinated product will be collected and treated in time, thereby reducing the corrosion of the reactor, improving the quality of the reaction product. Further, properly ensure that the reactor works in the micro-negative pressure to effectively avoid poisonous gas leakage [19].

At present, the pyrolysis processing of single plastics and specific proportions of mixed plastics has been studied fairly thoroughly. However, because there have been variations in the sources of the raw materials, the heat transfer limits and the data processing methods, the activation energy values obtained by different scholars have also varied greatly [20, 21]. Besides, the kinetic results of the same reaction process can vary, depending on the experimental conditions. Similarly, processing the kinetic data of thermal analysis at different heating rates can cause the activation energy results to be off by as much as 6%, even while using the same processing method (K-A-S) [22].

Plastic consumption also varies from region to region, and separating mixed plastics into individual ones requires high precision and efficient operation of the separation equipment, increasing the recycling costs. The complexity of waste plastic components prevents the wide application of pyrolysis because the technology and equipment are not always suitable for a particular type of plastic. Therefore, it is critical to fully research the kinetic parameters of waste plastic mixtures during the pyrolysis process. The thermal degradation of the mixture depends on the composition, structure and temperature of the individual polymer components, and the degradation is a mixture of series and parallel reactions rather than a superposition of component reactions [23].

A study of the pyrolysis process of PP and PVC mixtures has found that the activation energy required increases with the proportion of PVC. Generally, the addition of PP can hinder the dechlorination rate of PVC. Furthermore, the heat treatment process for chlorine-containing waste mixtures is more difficult than that for PVC [24, 25]. Many previous studies have focused mainly on the activation energy of the pyrolysis process while ignoring the influence of the pre-exponential factor and mechanism functions of the process. Under a high heating rate, the pyrolysis mechanism of PP can be described by a shrinking ball model. The pyrolysis mechanism of PVC, by contrast, is two-dimensional nucleation in the first stage and three-dimensional diffusion in the second stage [26]. However, higher heating rates cannot be applied in industrial production. Therefore, more research on the pyrolysis mechanism of mixed plastic components still needs to be carried out.

Model-free method and model-fitting method are commonly used to calculate the kinetic parameters of polymer pyrolysis process, wherein the kinetic parameters include activation energy, pre-exponential factor, and mechanism function. The activation energy can be easily obtained by the model-free method in the reaction process, but pre-exponential factor and mechanism functions are not easily obtained this way [27]. For the model-fitting method, a hypothetical response model is needed, if complete reaction kinetic parameters are desired [28]. Correspondingly, the solution process is relatively cumbersome and the basis for logical judgment of the mechanism function is sometimes insufficient. Therefore, in this study, a model-free method was used to determine the average activation energy of the reaction, as one of the bases for determining the statistical criterion for the mechanism functions. Furthermore, the results of the model-fitting method are comprehensively considered, to calculate complete kinetic parameters that can accurately express the reaction process. The solution process of the kinetic parameters of the mixture pyrolysis process is shown in Fig. 1.

Polystyrene (PS), often used for foam and fast-food containers, is one of the ingredients often found in plastic waste. In this study, a PP/PVC mixture and a PP/PVC/PS mixture were taken as samples of plastic wastes to be subjected to a pyrolysis process. Based on the actual production of plastic products, the kinetic parameters and pyrolysis principles of the two mixtures (PP/PVC and PP/PVC/PS) were compared and analyzed. In brief, a sustainable method of processing mixed plastic wastes is discussed here, and the article presents some ideas for solving the difficult problem of classification, sorting, and treatment of complex plastic wastes. It also provides theoretical support for the optimization of pyrolysis process parameters and the design of pyrolysis reactors for chlorine-containing mixed plastics.

Materials and methods

Materials and sample preparation

The three samples of plastic particles (PP, PVC and PS) used in the experiment were first purchased from the Branch Corporation of China Petroleum and Chemical (Yanshan, Beijing). The PP, PVC and PS plastic raw materials were dried at 105℃ for 12 h to remove the water contained in the materials and were crushed in a Huangdai 800Y high-speed multifunctional crusher (Zhejiang, China). Then, the powdered samples with a diameter of 80 mesh were used for Thermogravimetric Analysis (TGA). The mixed plastic samples were composed of the main components of typical Chinese plastic products—PP, PVC and PS. The ratio of each component in the sample is determined according to actual yield (Mass). The samples were weighed on a Precisa XB 220A balance (Switzerland). They were then mixed well, in
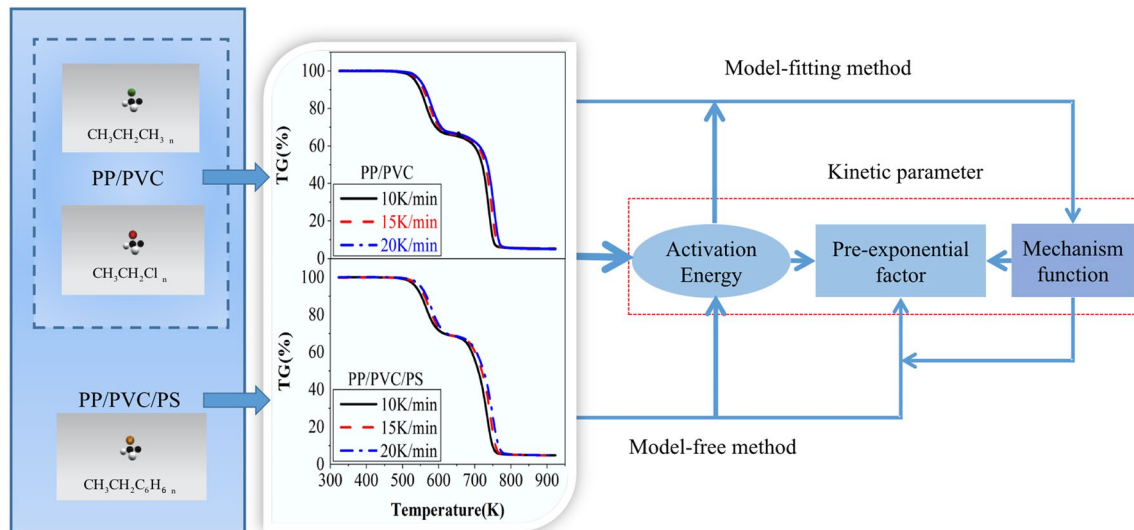
Fig. 1 Flow chart of the solution process of pyrolysis kinetic parameters of the mixture

proportion (PP: PVC = 7:6.2; PP: PVC: PS = 7:6.2:1), and put into a centrifuge tube for later use.

Characterization by Thermal Gravimetric Analyzer (TGA)

The pyrolysis was carried out in TG 209F3 from NETZSCH (Germany) under 99.9999% high-purity nitrogen. The flow was set to 50 ml/min with 20 ml/min nitrogen purge gas turned on. An aluminum crucible was used for the reaction vessel. Before the experiments, the machine was run for 2 h. After the standby device was stabilized, nitrogen purge gas was passed into the machine for 10 min. The experimental temperature was increased from 40 ℃ to 700 ℃, at heating rates of 10, 15 and 20 K/min. The mass of each sample in the experimental process was strictly controlled at 10 mg, which belongs to the optimal measuring range of TG equipment. Each group of experiments was repeated more than 3 times to obtain an average, to eliminate the interference of weather or human factors and ensure the reproducibility of the experimental curve.

Kinetic models

For the analysis of the pyrolysis kinetics of solid-phase systems, the iso-conversional method is a commonly used one. Multiple TG curves, which can determine the change in activation energy concerning conversion rate by the equal conversion rate method, were measured with thermogravimetric experiments, to reveal the complex nature

of the reaction [29]. Using the data at the same conversion rate on multiple TG curves measured at different heating rates, a more reliable activation energy value can be obtained without involving the kinetic model.

In the thermogravimetric analysis of a solid pyrolysis process, the conversion rate is defined as Eq. (1):

$$\alpha = (m_o - m_t)/(m_o - m_f) \qquad (1)$$

The kinetic equations of non-isothermal reactions commonly used in pyrolysis reactions can be described as follows:

$$\frac{d\alpha}{dt} = k(T)f(\alpha) \qquad (2)$$

The relationship between k and reaction temperature T can be explained by the Arrhenius equation:

$$k = A \exp(-E\alpha/RT) \qquad (3)$$

Incorporating Eq. (3) into Eq. (2), the kinetic equation under non-isothermal conditions is obtained:

$$\frac{d\alpha}{dT} = \frac{A}{\beta} \exp(-E\alpha/RT)f(\alpha) \qquad (4)$$

where, α is the conversion rate, %; m_o, m_t and m_f are the initial mass, the mass at time t, and the mass at the end of the sample, respectively, (mg); β is the heating rate, (K·min^{-1}); A is the pre-exponential factor; R is the gas constant, chosen as 8.314 J·mol^{-1}·K^{-1}; $E\alpha$ is the apparent activation energy, (kJ·mol^{-1}); T is the temperature of the reaction, (K); $f(\alpha)$ is the mechanism function in differential form.

Model-free method

The data processing method of the thermal analysis curve is divided into the integral method and the differential method. The integral method is represented by the Flynn–Wall–Ozawa (F–W–O) method, while the Kissinger–Akahira–Sunose (K–A–S) and the Starink method are often taken as representative in the differential method area[30–34]. The combination of the two methods could lead to more reliable kinetic parameters. The equations of these three analysis methods could be expressed by General Eq. (5):

$$\ln\left(\frac{\beta}{T^U}\right) = C_U - BE\alpha/RT \tag{5}$$

where $U = 2$, $B = 1$, $C_2 = \ln[A \cdot R/E\alpha \cdot G(\alpha)]$ in the K–A–S equation; $U = 1.8$, $B = 1.0037$, $C_{1.8} = \ln[A \cdot R/E\alpha \cdot G(\alpha)]$ in the Starink equation; $U = 0$, $B = 1.052$, $C_0 = \ln[A \cdot E\alpha/R \cdot G(\alpha)]$ in the F–W–O equation; $G(\alpha)$ is the mechanism function in integral form.

Model-fitting method

In non-isothermal kinetic analysis, the kinetic parameters of the same substance summarized by different researchers under the same experimental conditions often show large deviations. It is very important to choose a reasonable mechanism function logically because the selected mechanism function form might not fully explain the actual

kinetic process [29]. In this study, the method of combining Coats–Redfern (C-R) and Malek was used, to avoid the trouble of trying the mechanism functions one by one [35, 36].

The Malek method compares the degree of fit between the experimental data curve and the standard theoretical curve, to determine the kinetic reaction mechanism of the pyrolysis process [37].

From the reaction rate Eqs. (2), (3) and the C–R Eq. (6)

$$\int_0^\alpha \frac{d\alpha}{f(\alpha)} = G(\alpha) = \frac{1}{\beta}\frac{ART^2}{E\alpha}\exp(-E/RT) \tag{6}$$

Obtained

$$G(\alpha) = \frac{d\alpha}{dt}\frac{R}{\beta}\frac{T^2}{E\alpha}\frac{1}{f(\alpha)} \tag{7}$$

Putting $\alpha = 0.5$ into Eq. (7) and performing the division operation, the expression of the function $y(\alpha)$ can be defined:

$$y(\alpha) = \left(\frac{T}{T_{0.5}}\right)^2\frac{d\alpha/dt}{(d\alpha/dt)_{0.5}} = \frac{f(\alpha)G(\alpha)}{f(0.5)G(0.5)} \tag{8}$$

Values of conversion change with time at conversion α, $(d\alpha/dt)\alpha_i$, and temperature at conversion α_i, $T\alpha_i$, have been calculated at nine conversion values ($\alpha_i = 0.1, 0.2, ..., 0.9$). Thus, the left-hand side of Eq. (8) which was calculated from the experimental data was compared to the right-hand side term, defined according to the 19 kinetic functions described in Table 1 at the considered conversion levels.

Table 1 Solid pyrolysis kinetic functions commonly used

Reaction mechanism		Code	$f(\alpha)$	$G(\alpha)$
Power law	1	P_2	$\alpha^{1/2}$	$2\alpha^{1/2}$
	2	P_3	$\alpha^{1/3}$	$3\alpha^{2/3}$
	3	P_4	$\alpha^{1/4}$	$4\alpha^{3/4}$
Nucleation growth model	4	$A_{1/2}$	$[-\ln(1-\alpha)]^2$	$1/2(1-\alpha)[-\ln(1-\alpha)]^{-1}$
	5	A_1	$-\ln(1-\alpha)$	$(1-\alpha)$
	6	$A_{3/2}$	$[-\ln(1-\alpha)]^{2/3}$	$3/2((1-\alpha))[-\ln(1-\alpha)]^{1/3}$
	7	A_2	$[-\ln(1-\alpha)]^{1/2}$	$2((1-\alpha))[-\ln(1-\alpha)]^{1/2}$
	8	$A_{5/2}$	$[-\ln(1-\alpha)]^{5/2}$	$2/5((1-\alpha))[-\ln(1-\alpha)]^{3/5}$
	9	A_3	$[-\ln(1-\alpha)]^{1/3}$	$3((1-\alpha))[-\ln(1-\alpha)]^{2/3}$
	10	A_4	$[-\ln(1-\alpha)]^{1/4}$	$4((1-\alpha))[-\ln(1-\alpha)]^{3/4}$
Reaction order model	11	$F_{3/2}$	$2(1-\alpha)^{-3/2}$	$(1-\alpha)^{-1/2}$
	12	F_2	$(1-\alpha)^{-1}$	$(1-\alpha)^2$
	13	F_3	$(1-\alpha)^{-2}$	$1/2(1-\alpha)^3$
Shrinking core model	14	R_2	$1-(1-\alpha)^{1/2}$	$2(1-\alpha)^{2/3}$
	15	R_3	$1-(1-\alpha)^{1/3}$	$3(1-\alpha)^{1/2}$
Diffusion model	16	D_1	α^2	$1/2\alpha^{-1}$
	17	D_2	$\alpha+(1-\alpha)\ln(1-\alpha)$	$[-\ln(1-\alpha)]^{-1}$
	18	D_3	$[1-(1-\alpha)^{1/3}]^2$	$3/2(1-\alpha)^{2/3}[1-(1-\alpha)^{1/3}]^{-1}$
	19	D_4	$1-2/3\alpha-(1-\alpha)^{2/3}$	$3/2[(1-\alpha)^{2/3}-1]^{-1}$

Using this procedure, we found that many kinetic functions can describe the experimental data.

Reorganizing C–R Eq. (6) obtains:

$$\ln\left[\frac{G(\alpha)}{T^2}\right] = -\frac{E\alpha}{RT} + \ln\left[\frac{A}{\beta}\frac{R}{(E\alpha - 2RT)}\right] \tag{9}$$

For the pyrolysis temperature range and activation energy of plastics, $\ln\{A{\cdot}R/[\beta{\cdot}(E\alpha - 2RT)]\}$ is close to a fixed constant [20]. Hence, Eq. (9) can be treated as a linear equation $y = ax + b$, where, $a = 1/T$, $b = \ln\{A{\cdot}R/[\beta{\cdot}(E\alpha\text{-}2RT)]\}$.

Results and discussion

Thermodynamic analysis

Figure 2a, b shows the TG curves of the PP/PVC and PP/PVC/PS mixtures at heating rates of 10, 15 and 20 K/min. The pyrolysis reaction occurs into two steps, which are mainly related to the molecular structure of each component in the mixture. There is a gentle temperature plateau between the two steps. As the heating rate increases, the pyrolysis reaction moves to the high-temperature zone, and the plateau temperature section between the two reactions of the TG curve is shortened [29]. It can be seen from Table 2 that the separation of the multi-step pyrolysis reaction process of the mixture was facilitated in the slow heating rate stage. Meanwhile, the segmented collection and detection of gas-phase products produced in different reaction stages can be improved. Therefore, it is best to design the pyrolysis equipment for the pyrolysis of waste plastic mixtures with multi-stage reactions as a two-stage reactor, adopting a slow heating rate (10 K/min) in the first stage of the pyrolysis process and increasing the heating rate (20 K/min) in the second stage. In addition, the plateau temperature phase between the two reaction steps can be extended by 27.8%, thus avoiding the reaction lag phenomenon caused by entering a higher temperature range before the previous reaction has been completed [29]. The products of the two-stage pyrolysis reaction can be sorted and collected expeditiously. The pyrolysis process of the two mixtures is completed in two stages, depending mainly on the PVC content in the mixture [19]. When the heating rate is 10 K/min, the mass loss of the PP/PVC mixture in the first stage (531.95–588.75 k) is 24.54%, and it reaches
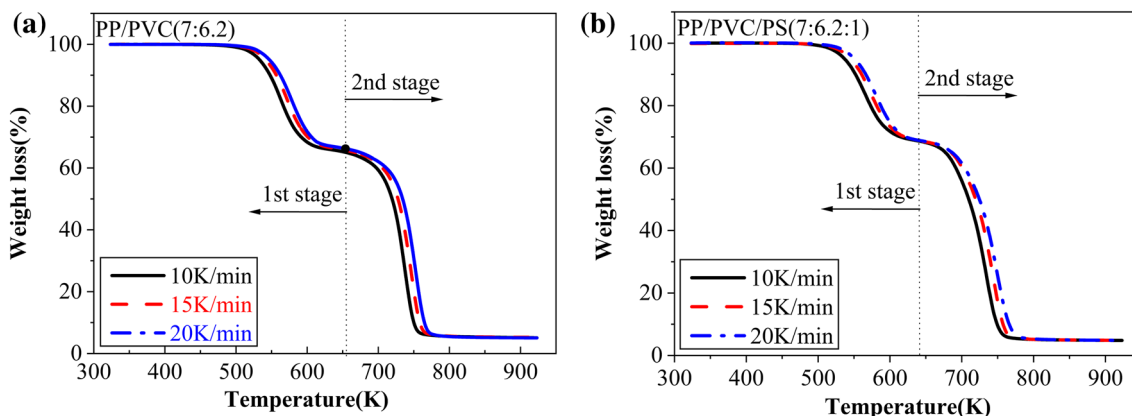

Fig. 2 TG curves of two mixtures under non-isothermal conditions

Table 2 Two-stage pyrolysis behavior of PP/PVC and PP/PVC/PS mixtures

Sample	Heating rate	Pyrolysis temperature interval								Residual mass
		1st stage				2nd stage				
	β(K/min)	T_{o1}(K)	T_{p1}(K)	T_{f1}(K)	S_1(%)	T_{o2}(K)	T_{p2}(K)	T_{f2}(K)	S_2(%)	C(%)
PP/PVC	10	531.95	562.25	588.75	24.54	717.65	737.85	750.55	41.68	4.99
	15	540.85	571.55	597.15	24.56	724.45	746.95	759.35	42.10	5.15
	20	549.75	578.15	604.55	24.84	730.15	749.25	764.85	42.98	5.23
PP/PVC/PS	10	532.85	564.75	591.25	22.35	702.85	733.75	750.05	46.36	4.81
	15	541.65	574.35	600.35	22.57	712.45	743.45	759.25	45.39	4.83
	20	547.35	580.75	607.15	23.16	716.95	749.15	766.65	44.70	4.87

41.68% in the second stage (717.65–750.55 k). The pyrolysis residual mass for the whole pyrolysis process is 4.99%. Correspondingly, the mass loss of the PP/PVC/PS mixture is 22.35% in the first stage of pyrolysis (532.85–591.25 k) and reaches 46.36% in the second stage (702.85–750.05 k) with a 4.81% residual mass for the whole pyrolysis process. In the first stage of the pyrolysis, the only dechlorination of the PVC occurs, producing a large amount of hydrogen chloride gas [38]. The second stage of the reaction process is more complicated, because of the fracture of the polyene conjugate structure and the crosslinking, isomerization and aromatization of pyrolysis products[12, 39]. Moreover, the dehydrochlorination seems to be complete before the decomposition of the other polymers begins and it appears that there are no reactions of hydrogen chloride with the second polymer [40]. However, the results show that the chlorine release of the PP/PVC/PS blend was postponed, indicating an antagonistic effect during the pyrolysis. PS appears to be responsible for the shift of TG curves of polyolefins towards low decomposition temperatures while PS itself in the mixture is stabilized [41]. This may be because the addition of PS increases the dispersion of PVC aggregates in the mixture, and the thermal conductivity of PS is worse than that of PVC, which weakens the heat transfer effect between the mixtures and hinders the progress of the dechlorination reaction (the thermal conductivity of PS and PVC are 0.08 and 0.16 W/m·k, respectively). Furthermore, intermolecular hydrogen transfer might be the predominant reaction between components of the polymer mixtures [42]. The addition of PS has a synergistic effect on the second-stage pyrolysis of the mixture, which causes the pyrolysis reaction of the mixture to proceed earlier. Comparing the heating rates of 15 and 20 K/min, the mass loss ratio in the first stage increases and the pyrolysis temperature range widens with the increase of the heating rate, while the mass loss in the second stage decreases and the residual mass increases slightly.

When the heating rate is 10 K/min, the two-peak pyrolysis rates of the PP/PVC mixture are 5.89 and 16.53%/min, while for the PP/PVC/PS mixture, the rates are 5.09 and 12.94%/min. The comparison of the two mixtures shows that the addition of PS will slow down the pyrolysis rate of the two stages. Specifically, the peak rate of the dechlorination process in the first stage was reduced by 16%, and the peak pyrolysis rate in the second stage was reduced by 27.7%, which was related primarily to the heat transfer effect and interaction between the internal components of the mixture. The dechlorination reaction is gradual in the first stage, and the best dechlorination temperatures for the two mixtures are 562.25 K (PP/PVC) and 564.75 K (PP/PVC/PS). The macromolecular chain scission reaction process is more violent in the second stage; 737.85 K (PP/PVC) and 733.75 K (PP/PVC/PS) are better pyrolysis temperatures. In addition, the peak pyrolysis rate of the two-stage reaction keeps rising with the increase in the heating rate (Supplementary Information Fig. S1).

Kinetic analysis

Model-free methods

The thermogravimetric data of the three heating rates were substituted into Eq. (5), the ln (β/T^2), ln $(\beta/T^{1.8})$ and ln (β) VS $1/T$ curves were plotted in the Origin software at equal conversion rate ($\alpha_i = 0.1$, 0.2…, 0.9), and then the least square method was used to perform linear fitting treatment on the curves. Finally, the activation energy was calculated according to the slope of the fitting line, the relevant parameters are shown in Fig. S2 of the Supplementary Information.

Previous studies have shown that in some binary mixtures an interaction can occur between the components, resulting in variations in each composition kinetic parameter. Under nitrogen atmosphere, retardation of PP in PVC/PP mixtures was observed by compared apparent activation energies of binary mixtures [43, 44]. Comparing the calculation results for average activation energy (A_V) of the two mixtures from Table 3, it can be found that the addition of PS has little effect on the activation energy of the first-stage pyrolysis reaction. However, it significantly reduces the activation energy of the second-stage reaction because the pyrolysis

Table 3 Kinetic parameters obtained by model-free methods (K–A–S, Starink and F–W–O) at different heating rates

Sample	Segmented		K-A-S		Starink		F-W-O	
			E_i	A_i	E_i	A_i	E_i	A_i
PP/PVC	1st stage	Range	109.4–116.1	3.76E+06–2.20E+07	109.9–116.7	1.63E+07–8.85E+07	112.8–119.8	1.85E+15–1.14E+16
		A_V	113.4	1.26E+07	116.7	8.85E+07	116.7	6.36E+15
	2nd stage	Range	216.8–226.0	9.88E+11–4.56E+12	217.3–226.4	4.54E+12–2.08E+13	218.1–226.6	8.72E+20–3.91E+21
		A_V	220.3	2.26E+12	220.7	1.04E+13	221.7	1.97E+21
PP/PVC/PS	1st stage	Range	108.1–116.2	2.58E+06–2.17E+07	108.7–116.8	1.14E+07–8.03E+07	111.5–119.8	1.25E+15–1.01E+16
		A_V	112.8	1.17E+07	113.4	4.66E+07	116.2	5.59E+15
	2nd stage	Range	178.0–191.1	1.69E+09–1.83E+10	178.6–191.8	7.75E+09–8.16E+	188.0–193.7	5.01E+18–1.56E+19
		A_V	188.5	1.34E+10	189.0	5.80E+10	192	1.18E+19

temperature intervals of PP and PS may not overlap with those of the PVC dechlorination process. In the second stage of the pyrolysis process, a complex reaction occurs among PP, PVC and PS. The activation energy among the three components is $\{PVC\}_2 > PP > PS$ (the subscript 2 for PVC refers to the second stage of pyrolysis). The activation energies obtained by the three methods are relatively stable during the two stages of the pyrolysis reaction, but the average activation energy between the two stages of the reactions is quite different, a result that also verifies that the pyrolysis process of the mixture is carried out in two steps. The average activation energy ranking of the step reaction is F–W–O > Starink > K–A–S, which is consistent with conclusions drawn in the literature [45]. The molecular structure is an important factor affecting activation energy. PS has a higher degree of branching, so the energy required for chain scission in mixtures containing PS is reduced thereby reducing the overall activation energy of the mixture. Moreover, the interaction between the mixed components may also play an important role. However, the fracture of the polyene conjugate structure and the crosslinking, isomerization and aromatization of pyrolysis products, in terms of activation energy, is beneficial to the pyrolysis of the mixture. The analysis results are also consistent with the analysis results of the pyrolysis behavior of the mixture. A recent work by Knumann and Bockhorn reported no significant interaction between mixtures of PVC with polyolefins compared with TG/DTG theoretical curves based upon the behavior of individual polymers.

Model-fitting methods

The experimental data curve and the standard data curve are drawn in the Origin software, and the equation that can make the experimental data curve consistent with the standard data curve is screened out from the 19 equations in Table 1,

these mechanism functions will be further confirmed by the Eq. (9). As shown in Fig. 3a, b, comparing the experimental and theoretical curves of the pyrolysis reaction data, it can be found that the first-stage pyrolysis reaction of the PP/PVC and PP/PVC/PS mixtures is more suitable for the function numbered 4, 5, 6, 7, 8, 9, and 10.

When the mass loss is 10–80%, the second stage is also close to the mechanism function of these equations, which belong to the Random nucleation and subsequent growth. However, when the mass loss exceeds 80%, it inclined to the function numbered 15 and 18, which appertain to the three-dimensional diffusion(D_3) and the phase boundary reaction Shrinking sphere(R_3). However, the theoretical curve with the higher fit of the two-step reaction data corresponds to multiple equations, making it impossible to determine the applicable function equations and requiring further research.

The statistical criterion of mechanism function $G(\alpha)$: (1) The mechanism function which can obtain the higher coefficient of determination by fitting curves in C–R equation; (2) The mechanism function which can obtain the similar activation energy by model-free method (C–R) and model-free method (K–A–S, Starink and F–W–O). The $G(\alpha)$ which can satisfy the above two requirements is the most probable mechanism function of the reaction process. The specific procedures are as follows: The undetermined integral function form $G(\alpha)$ of the Malek method and thermogravimetric experimental data can be plugged into the C-R equation. The $\ln[G(\alpha)/T^2]$ VS $1/T$ curves were drawn with Origin software, and the curves were fitted with the least squares.

As presented in Table 4, the model-fitting (C–R) method was applied at the heating rate of 10 K/min to determine the values of the activation energy and the degradation mechanism of two mixtures.

It is clearly shown that there is no significant difference in the coefficient of determination (R^2) under different mechanism functions. However, when the mechanism for
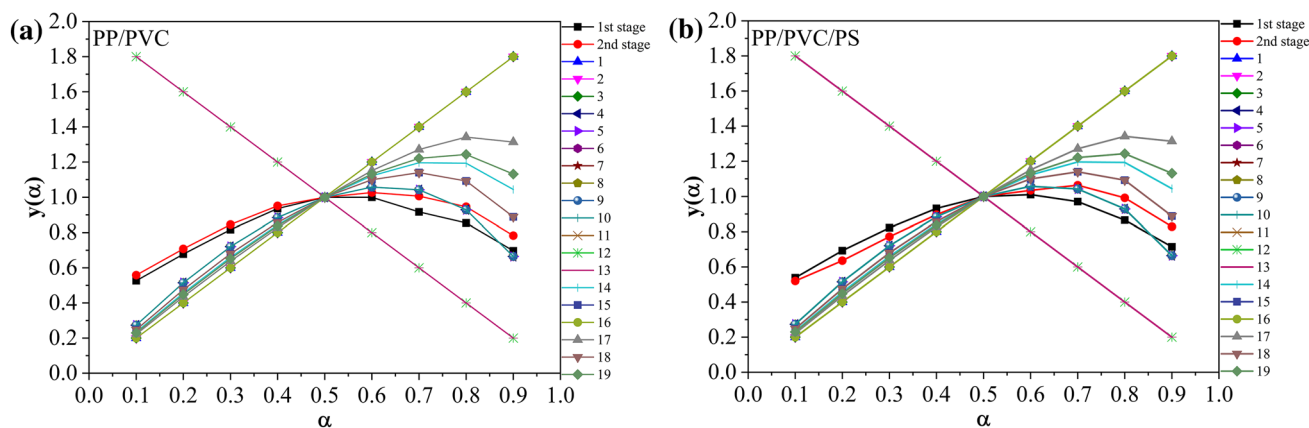

Fig. 3 Comparison curve of thermogravimetric data and theoretical data of the two-stage reaction for the mixture

Table 4 Kinetic parameters of the two mixtures under different mechanisms were obtained by the C–R method (10 K/min)

Reaction stage	Mechanism code	PP/PVC			PP/PVC/PS		
		E_i	A_i	R_2	E_i	A_i	R_2
1st stage	$A_{1/2}$	376.2	5.96E+31	0.988	366.9	4.91E+31	0.987
	A_1	183.5	5.24E+13	0.988	178.8	1.35E+14	0.987
	$A_{3/2}$	119.2	4.16E+07	0.987	116.1	1.56E+09	0.986
	A_2	87.1	3.35E+04	0.986	84.7	2.24E+07	0.985
	$A_{5/2}$	67.8	4.40E+02	0.985	65.9	1.52E+05	0.984
	A_3	54.9	2.34E+01	0.984	53.4	1.28E+02	0.983
	A_4	38.9	5.50E−01	0.982	37.7	3.31E+00	0.981
2nd stage	$A_{1/2}$	1126.6	1.09E+77	0.989	755.2	7.93E+51	0.995
	A_1	557.1	2.99E+36	0.989	371.5	1.92E+24	0.994
	$A_{3/2}$	367.4	7.57E+22	0.989	243.7	9.97E+14	0.994
	A_2	272.5	1.10E+16	0.988	179.7	2.06E+10	0.994
	$A_{5/2}$	215.6	8.22E+11	0.988	141.4	3.03E+07	0.994
	A_3	177.6	1.40E+10	0.988	115.8	3.75E+05	0.993
	A_4	130.1	4.55E+06	0.987	83.8	1.44E+03	0.993
	D_3	483.7	4.45E+30	0.967	322.7	1.47E+20	0.976
	R_3	1002.7	1.29E+67	0.977	673.0	7.45E+44	0.986

{PP/PVC}$_1$ and {PP/PVC/PS}$_1$ degradation is proposed to be A$_{3/2}$ type (The subscript 1 for PP/PVC and PP/PVC/PS refers to the first stage of pyrolysis), the calculated activation energy of this mechanism was around 116.1–119.2 kJ/mol using C–R method, which was similar to the average activation energy obtained by the model-free method (113.4–116.7 kJ/mol). Therefore, random nucleation followed by growth (A$_{3/2}$) is the most probable mechanism function of two mixtures in the first pyrolysis stage. The nucleation mechanism represents the formation of new product phases at certain, reaction points (nucleation sites) in the reactant lattice [46]. Obtained model of the dechlorination stage also resembles the reaction models reported by Wu and Xu et al. However, for the second phase of PVC pyrolysis, the conclusion of the reaction mechanism is still inconsistent [26, 41].

The second pyrolysis stage of the chlorine-containing mixture is very complicated, it can be driven by the dominant reactions between the degradation products from {PVC}$_2$ and PP. From the DTG curves of two mixtures, only one pyrolysis peak is found in the second stage of each pyrolysis process, indicates that the complex reaction is close to a dominant reaction, although it may be jointly promoted by multiple reaction mechanisms. When the dominant reaction is strong enough to be close to the actual reaction process, the dominant reaction can be used as the degradation mechanism. When the mechanism function of {PP/PVC}$_2$ is proposed to be A$_{5/2}$, the calculated activation energy of this mechanism was around 215.6 kJ/mol using the C-R method, while the average activation energy obtained by the model-free method (220.3–221.7 kJ/mol). The deviation range of the activation energy value under

the two methods is completely acceptable. Similarly, the thermal degradation mechanism of {PP/PVC/PS}$_2$ is proposed to be of A$_2$ type. (The subscript 2 for PVC, PP/PVC and PP/PVC/PS refer to the second stage of pyrolysis). In the mechanism code 'A$_{3/2}$ and A$_{5/2}$', 'A' refers to the mechanism of random growth after fluvial formation, and subscript '3/2 and 5/2'is kinetic indices.

Figure 4a, b shows the fitting results of experimental data and the most probable mechanism function in the first stage of pyrolysis, and c, d shows the fitting results of experimental data and the most probable mechanism function in the second stage of pyrolysis.

Mechanism model verification

Two approaches were applied to verify the accuracy of the kinetic model above mentioned. The first approach involved a comparison of the experimental TG/DTG curve with a calculated curve. The second approach involved a comparison of the kinetic parameters determined by model-free and model-fitting methods. Thermogravimetric experiments of the two mixtures were carried out at a heating rate of 30 K/min under the same experimental conditions. The experimental data and the determined mechanism function $G(a)$ were substituted into the C–R equation, and the kinetic parameters obtained were shown in Table 5.

For the two samples of this research, the integral form of mechanism functions can be expressed as:

$$f(a) = (1-a)^n$$

Equation (6) upon integration becomes:

Fig. 4 The fitting curve of experimental data and the most probable mechanism function in the two-stage of pyrolysis (10 K/min)
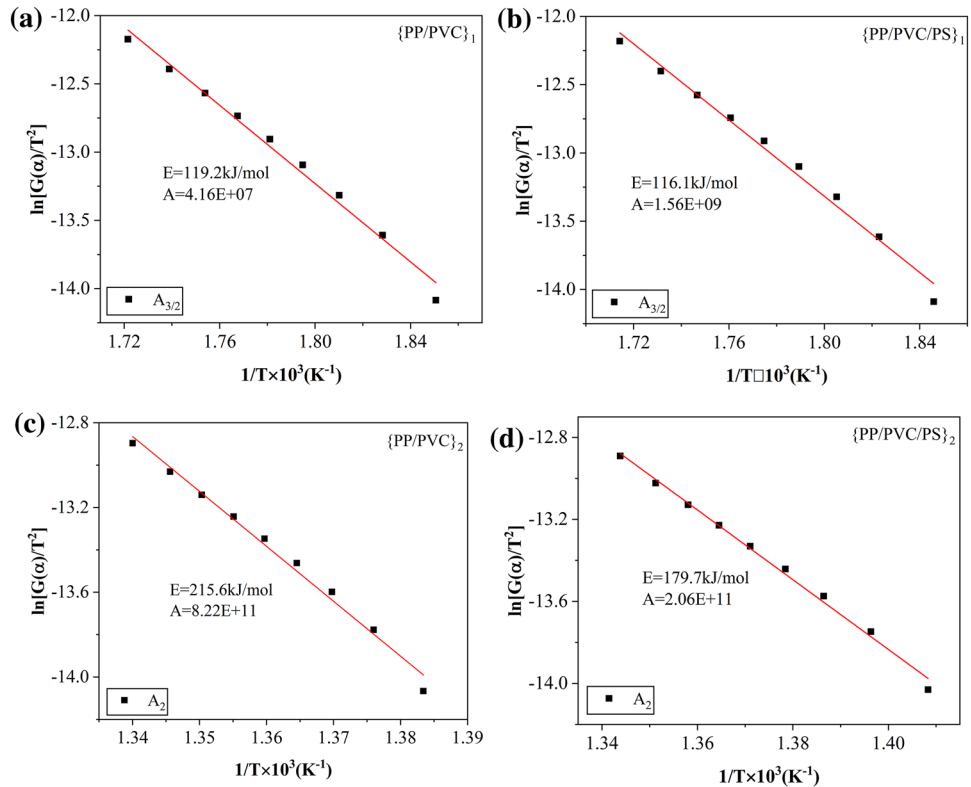

Table 5 Kinetic parameters for two mixtures at a heating rate of 30 K/min

Sample	1st stage				2nd stage			
	$E\alpha$(kJ·mol^{-1})	A (min^{-1})	n	$r(\%)$	$E\alpha$(kJ·mol^{-1})	A (min^{-1})	n	$R(\%)$
PP/PVC	122.8	8.78E+07	1.5	37.06	201.5	2.26E+11	2.5	32.53
PP/PVC/PS	120.4	4.41E+07	1.5	62.94	214.3	8.2E+11	2	67.47

$$\int_0^\alpha \frac{d\alpha}{(1-\alpha)^n} = \frac{A}{\beta}\int_{T_f}^{T_f} e^{-E\alpha/RT}dT = \frac{AE\alpha}{\beta R}p(x) \qquad (10)$$

where $x = E\alpha/(RT)$. It is assumed that T_o is low enough for the lower limit to be negligible.

For n ≠ 1:

$$\frac{(1-\alpha)^{1-n}-1}{1-n} = -\frac{AE\alpha_i}{\beta R}P(x) \qquad (11)$$

To calculate $p(x)$, we have chosen to use Lyon's approximation:

$$P(x) = \frac{e^x}{x(x-2)} \qquad (12)$$

The simplest way to model the TG curves is to consider the two weight loss stages involved in the degradation as an independent. Therefore, the overall rate of conversion is given by [47]:

$$1-\alpha = 1 - \sum_{i=1}^{2} r_i\alpha_i$$

$$= 1 - \sum_{i=1}^{2} r_i \left\{ 1 - \left[1 - (1-n_i)\frac{A_i RT^2}{\beta(E\alpha_i + 2RT)} \exp\left(-\frac{E\alpha_i}{RT}\right) \right]^{\frac{1}{1-n_i}} \right\}$$

(13)

In this expression, r_i is the yield coefficient of the ith weight-loss stage with $r_i < 1$ and $\sum_{i=1}^{2} r_i = 1$

The activation energies of the two verification tests under the mechanism function are in good agreement with the results of the model-free method. Moreover, the results of the final kinetic models along with the original TGA data are given in Fig. 5. A good agreement with

Fig. 5 Simulated TG curves for two mixtures at a heating rate of 30 K/min
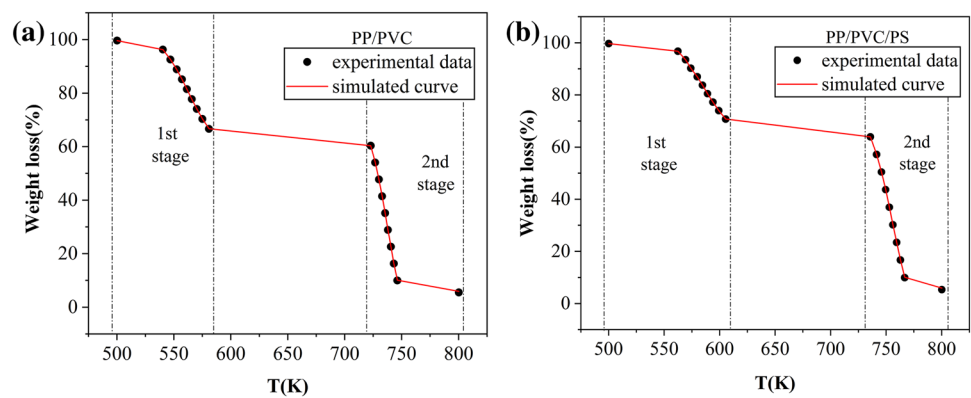
experimental data demonstrates that the mechanism models are valid representations of the underlying physics.

With the mechanism function determined, the pre-exponential factors of the three model-free methods (K–A–S, Starink and F–W–O) were calculated; thus, the complete kinetic parameters were presented in Table S1 of the supplementary information. It can be seen that the exponential pre-factors of the two-step reactions obtained by the K–A–S and Starink methods are highly similar, while the pre-exponential factors obtained by the F–W–O method are noticeably higher.

Conclusion

Thermogravimetric experiments were performed on two mixtures—PP/PVC and PP/PVC/PS—under non-isothermal conditions. Pyrolysis characteristics and kinetic parameters of the mixtures were studied by the multiple rate scanning method. From the thermogravimetric curve, it can be found that the pyrolysis process of the two mixtures can be divided into two stages. The dechlorination temperature can be reduced and the temperature plateau between the two reactions can be extended, when combining low heating rates with high heating rates for the separation of pyrolysis products. Three model-free methods (K–A–S, Starink and F–W–O) were carried out to obtain the two-stage stable activation value of the mixture's pyrolysis processes. The average valves of activation energy for the two-stage pyrolysis reaction of the PP/PVC mixture were 114.7 kJ/mol in the first stage and 220.9 kJ/mol in the second stage, while the corresponding values for PP /PVC/PS were 114.7 kJ/mol and 189.8 kJ/mol, respectively.

Model-free and model-fitting methods are taken as the logical bases for determining the pyrolysis principle. Varying pyrolysis characteristics for the two mixtures are obtained when the heating rate is 10 K/min: for both {PP/PVC}$_1$ and {PP/PVC/PS}$_1$, the pyrolysis mechanism is random nucleation followed by growth A$_{3/2}$; for {PP/PVC}$_2$, the pyrolysis mechanism is random nucleation followed by growth A$_{5/2}$; for {PP/PVC/PS}$_2$, the pyrolysis mechanism is random nucleation followed by growth A$_2$. Moreover, the pre-exponential factor of the model-free method is determined under the guidance of the mechanism function. The comparison results of the two mixtures show that the additional PS causes some changes to pyrolysis regularity. Although there is no obvious influence on the activation energy or pyrolysis characteristics in the first phase, the activation energy in the second phase is reduced. For practical application, however, more research on the pyrolysis process of mixed plastic wastes is still needed, to improve the operational efficiency.

References

1. Ma ZF, Jiang WJ, Yang S (2019) China plastics processing industry (2018). China Plast 33(06):127–131
2. Al-Salem SM, Antelava A, Constantinou A (2017) A review on thermal and catalytic pyrolysis of plastic solid waste (PSW). Environ Manag 197:177–198
3. Chen WQ, Ciacci L, Sun NN (2020) Sustainable cycles and management of plastics: a brief review of RCR publications in 2019 and early 2020. Resour Conserv Recycl 159:104822
4. Barnes DKA, Galgani F, Thompson RC (2009) Accumulation and fragmentation of plastic debris in global environments. Philos Trans R Soc B: Biol Sci 364(1526):1985–1998

5. Lee S, Yoo SK, Lee J et al (2009) Hydrogen-rich fuel gas production from refuse plastic fuel pyrolysis and steam gasification. J Mater Cycles Waste Manag 11(3):191–196

6. Geyer R, Jambeck JR, Law KL (2017) Production, use, and fate of all plastics ever made. Sci Adv 3(7):1700782–1700782

7. World Economic Forum, MC Foundation and McKinsey Company (2016) The new plastics economy-rethinking the future of plastics. http://www.ellenmacarthurfoundation.org/publications

8. National Bureau of Statistics (2019) Statistical bulletin of the people's republic of China on the 2018 National economic and social development. China Stat (03):8–22

9. Gunasee SD, Carrier M, Mohee R (2016) Pyrolysis and combustion of municipal solid wastes: evaluation of synergistic effects using TGA-MS. J Anal Appl Pyrol 121:50–61

10. Anuar Sharuddin SD, Abnisa F, Daud WMAW (2017) Energy recovery from pyrolysis of plastic waste: study on non-recycled plastics (NRP) data as the real measure of plastic waste. Energy Convers Manag 148:925–934

11. Kumagai S, Yoshioka T (2016) Feedstock recycling via waste plastic pyrolysis. J Jpn Pet Inst 59(6):243–253

12. Williams PT, Slaney EJ (2007) Analysis of products from the pyrolysis and liquefaction of single plastics and waste plastic mixtures. Resour Conserv Recycl 51(4):754–769

13. Nanda S, Berruti F (2021) Thermochemical conversion of plastic waste to fuels: a review. Environ Chem Lett 19(1):123–148

14. Kumar A, Sharma MP (2014) GHG emission and carbon sequestration potential from MSW of Indian metro cities. Urban Clim 8:30–41

15. Vasile C, Brebu MA, Karayildirim T et al (2006) Feedstock recycling from plastic and thermoset fractions of used computers (I): pyrolysis. J Mater Cycles Waste Manag 8(2):99–108

16. Owusu PA, Banadda N, Zziwa A et al (2018) Reverse engineering of plastic waste into useful fuel products. J Anal Appl Pyrol 130:285–293

17. Naqvi SR, Prabhakara HM, Bramer EA (2018) A critical review on recycling of end-of-life carbon fibre/glass fibre reinforced composites waste using pyrolysis towards a circular economy. Resour Conserv Recycl 136:118–129

18. Yu J, Sun LS, Jie M et al (2016) Thermal degradation of PVC: a review. Waste Manag 48:300–314

19. Lopez A, de Marco I, Caballero BM et al (2011) Dechlorination of fuels in pyrolysis of PVC containing plastic wastes. Fuel Process Technol 92(2):253–260

20. Liu YB, Ma XB, Chen DZ (2010) Co-pyrolysis characteristics and kinetics analysis of typical waste plastics. Proc CSEE. 30:56–61

21. Qiao YY, Wang B, Zong PJ (2019) Thermal behavior, kinetics and fast pyrolysis characteristics of palm oil: analytical TG-FTIR and Py-GC/MS study. Energy Convers Manag 199:104887

22. Diza Silvarrey LS, Phan AN (2016) Kinetic study of municipal plastic waste. Int J Hydrog Energy 41(37):16352–16364

23. Tuffi R, D'Abramo S, Cafiero LM, Trinca E (2018) Thermal behavior and pyrolytic degradation kinetics of polymeric mixtures from waste packaging plastics. Polym Sci 12(1):82–99

24. Ahmad Z, Al-Sagheer F, Al-Awadi NA (2009) Pyro-GC/MS and thermal degradation studies in polystyrene-poly (vinyl chloride) blends. J Anal Appl Pyrol 87(1):99–107

25. Yuan ZL, Zhang J, Zhao PT (2020) Synergistic effect and chlorine-release behaviors during co-pyrolysis of LLDPE, PP, and PVC. ACS Omega 5(20):11291–11298

26. Xu FF, Wang B, Yang D (2018) Thermal degradation of typical plastics under high heating rate conditions by TG-FTIR: pyrolysis behaviors and kinetic analysis. Energy Convers Manag 171:1106–1115

27. Chowlu ACK, Reddy PK, Ghoshal AK (2009) Pyrolytic decomposition and Model-free kinetics analysis of mixture of polypropylene (PP) and low-density polyethylene (LDPE). Thermochim Acta 485(1–2):20–25

28. Zhou R, Huang BQ, Ding YM (2019) Thermal decomposition mechanism and kinetics study of plastic waste chlorinated polyvinyl chloride. Polymers 11(12):103390

29. Liu ZH, Zhang HL (2016) Thermal analysis and calorimetry, vol 64. Chemical Industry Press, Beijing, pp 56–79

30. Cafiero L, Castoldi E, Tuffi R (2014) Identification and characterization of plastics from small appliances and kinetic analysis of their thermally activated pyrolysis. Polym Degrad Stab 109:307–318

31. Chen L, Wang SZ, Meng HY (2017) Synergistic effect on thermal behavior and char morphology analysis during co-pyrolysis of paulownia wood blended with different plastics waste. Appl Therm Eng 111:834–846

32. Liu H, Chen B, Wang C (2020) Pyrolysis kinetics study of biomass waste using shuffled complex evolution algorithm. Fuel Process Technol 208:106509

33. Yao Z, Yu S, Su W et al (2020) Kinetic studies on the pyrolysis of plastic waste using a combination of model-fitting and model-free methods. Waste Manag Res 38(1_suppl):77–85

34. Rasam S, Haghighi AM, Azizi K (2020) Thermal behavior, thermodynamics and kinetics of co-pyrolysis of binary and ternary mixtures of biomass through thermogravimetric analysis. Fuel 280:118665

35. Hu Q, Tang ZY, Yao DD (2020) Thermal behavior, kinetics and gas evolution characteristics for the co-pyrolysis of real-world plastic and tyre wastes. J Clean Prod 260:121102

36. Zhu YL, An J, Chang H (2020) An analytical method for overlapping of the melting and decomposition of 2-oximemalononitrile. J Therm Anal Calorim 11:1–7

37. Hu RZ, Gao SL, Zhao FQ (2008) Thermal kinetics. Science Press, Beijing

38. Tondl G, Bonell L, Pfeifer C (2018) Thermogravimetric analysis and kinetic study of marine plastic litter. Mar Pollut Bull 133:472–477

39. Yu J, Sun L, Ma C et al (2016) Thermal degradation of PVC: a review. Waste Manag 48:300–314

40. Miranda R, Yang J, Roy C et al (2001) Vacuum pyrolysis of commingled plastics containing PVC I Kinetic study. Polym Degrad Stab 72(3):469–491

41. Wu J, Chen T, Luo X et al (2014) TG/FTIR analysis on co-pyrolysis behavior of PE PVC and PS. Waste Manag 34:676–682

42. Dodson B, McNeill IC (1976) Degradation of polymer mixtures. VI. Blends of poly(vinyl chloride) with polystyrene. J Poly Sci Polym Chem Ed 14(2):353–364

43. Day M, Cooney JD, Klein C (1993) Degradation behaviour of polymeric materials found in auto Shredder residue wastes. J Therm Anal 40:669–676

44. Day M, Cooney JD, Fox JL (1994) The use of thermogravimetry to analyze a mixed plastic waste stream. J Therm Anal 42(2–3):397–424

45. Wu GQ, Li J, Xu ZM (2013) Triboelectrostatic separation for granular plastic waste recycling: a review. Waste Manag 33(3):585–587

46. Khawam A, Flanagan DR (2010) Solid-state kinetic models: basics and mathematical fundamentals. J Phys Chem B 110(47):17315–21732

47. Ferriol M, Gentilhomme A, Cochez M et al (2003) Thermal degradation of poly (methyl methacrylate) (PMMA): modeling of DTG and TG curves. Polym Degrad Stab 79(2):271–281